Effect of alkyl chain length in protic ionic liquids: an AIMD perspective

M. Campetella, M. Macchiagodena, L. Gontrani & B. Kirchner

⊞ View supplementary material ↗

📅 Published online: 03 Apr 2017.

✎ Submit your article to this journal ↗

📊 Article views: 122

🔍 View related articles ↗

◯ View Crossmark data ↗

🗐 Citing articles: 3 View citing articles ↗

Taylor & Francis
Taylor & Francis Group

RESEARCH ARTICLE

Check for updates

Effect of alkyl chain length in protic ionic liquids: an AIMD perspective

M. Campetella [a], M. Macchiagodena[b], L. Gontrani[a] and B. Kirchner[b]

[a]Dipartimento di Chimica, Sapienza Università di Roma, Piazzale Aldo Moro, Rome, Italy; [b]Mulliken Center for Theoretical Chemistry, Institut für Physikalische und Theoretische Chemie, Universität Bonn, Beringstraße, Bonn, Germany

ABSTRACT

In this study we have explored, by means of *ab initio* molecular dynamics, a subset of three different protic ionic liquids (ILs). We present both structural and dynamical information of the liquid state of these compounds as revealed by accurate *ab initio* computations of the interactions. Our analysis figures out the presence of a strong hydrogen bond network in the bulk state, that is more stable in those ILs characterised by a longer alkyl side chain. Indeed it becomes more long-lasting passing from ethyl ammonium to butyl ammonium, owing to the hydrophobic effects stemming from alkyl chain contacts. Furthermore, the relative free energy landscape of the cation–anion interaction exhibits a progressively deeper well as the side chain of the cation gets longer. The hydrogen bond interaction, as already mentioned in previous works, leads to loss of degeneracy of the asymmetric stretching vibrations of the nitrate anions. The resulting frequency splitting between the two normal modes is about 90 cm^{-1}.
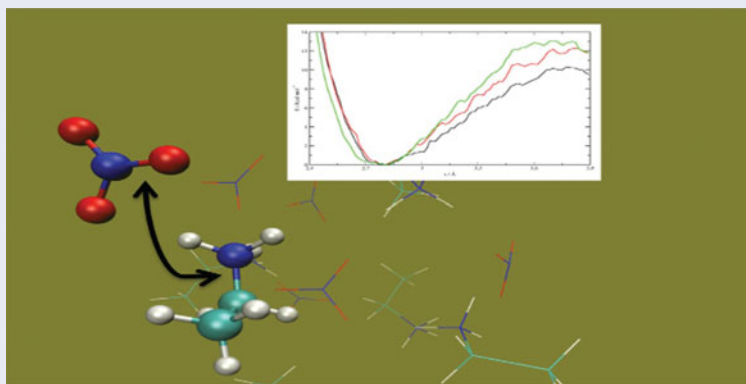
1. Introduction

Ionic liquids (ILs) constitute a class of useful and interesting materials, that are currently object of wide research, both fundamental and applicative [1–3]. Among the properties they are provided with, the well-known low-vapour pressure [4] and high thermal and chemical stability [5] make them optimal substitutes for typically polluting volatile organic solvents (VOC), furthermore a new generation of low toxic ILs for human and plants have been recently synthesised [6]. An interesting subset of ionic liquids are protic ionic liquids that can be synthesised by combining Brönsted acids and bases [7]. Proton transfer from the acid (donor) to the base (acceptor) leads to the formation of a pure liquid made up of ion pairs where proton acceptor and donor sites eventually generate a hydrogen-bond network [8–10]. Among protic ionic liquids, we studied the following systems: ethylammonium nitrate (EAN) [11], propylammonium nitrate (PAN) [12] and butylammonium nitrate (BAN) [13] (see Figure 1).

They are *N*-alkyl ammonium salts, containing the same anion (Ani), nitrate and a variable cation (Cat) which differs for the length of the alkyl chain bonded to the ammonium group. The strong hydrogen bond formed between the N–H$^+$ donor and the $^-$O–N acceptor groups is the main driving force responsible for the molecular aggregation of the condensed phase. Regarding the nitrate group, it is well known [14] that the free anion has planar structure, having D_{3h} symmetry and six
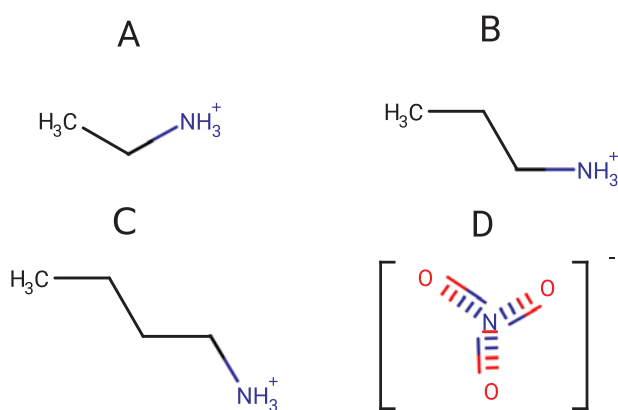
Figure 1. Sketch of the cations and the anion: (a) ethylammonium, (b) propylammonium, (c) butylammonium and (d) nitrate.

normal modes: the (ν_1) in-plane deformation, the (ν_2) out-of-plane deformation, the (ν_3) asymmetric stretching and the (ν_4) totally symmetric stretching (ν_1 and ν_3 are doubly degenerate). A recent work [15] about nitrate in liquid phase has shown the effects of symmetry breaking on the vibrations of the anion when point symmetry reduces from D_{3h} to C_{2v} up to C_s. The band due to ν_3 mode of the anion splits into two different components; furthermore, it exhibits a broad shape when measurements are made in a polar solvent. Moreover, the presence of hydrogen bonds in the liquid causes the band broadening of N–H stretching [11]. In addition to this aspect, recent works have figured out [16] how hydrogen bond might be a valuable source of disorder in the condensed phase of ionic liquids [9]. For example, it has been shown in a previous *ab initio* molecular dynamics (AIMD) study on methylammonium nitrate (MAN) [17] that the hydrogen bond network is not complete or saturated, and that roughly just two of the three oxygen atoms of the nitrate are involved in (strong) hydrogen bonds. This might be the consequence of strong polarisation and many-body effects. When such effects come into play, it is extremely difficult to provide valuable computational results using a pairwise potential like those commonly employed by most classical MD simulation programs. This issue is actually crucial because structural and dynamical observables, such as radial distribution functions (RDFs) and velocity autocorrelation functions (VAFs), are heavily dependent on them [18]. In this view, it is hardly possible to obtain reliable results for these properties with classical molecular dynamics as it is, instead, in less complex compounds [19]. For example, previous works have shown the requirement to build an *ad hoc* two-body potential (not transferable to other systems) [20] or a general three-body potential energy term [21] in order to reach a reasonable representation of the pair correlation function in such ILs. For

this reason it is necessary to go beyond this computational approach and to adopt a more sophisticated model [22–25]. We propose in this paper an *ab initio* molecular dynamics (AIMD) study, in order to interpret the structure of the corresponding bulk liquid systems focusing on the structural characteristics of the H-bonding network. Due to the limited size of the box currently affordable with AIMD, we cannot describe the medium-long order present [20,26] in these ILs, and our exploration is limited to short distances only. For the sake of providing the effects of the cation alkyl chains length for this subset of protic ILs, we have performed different analyses. We extracted some important static parameters, and subsequently we focused our attention on dynamic and energetic quantities. Furthermore, we performed the vibrational study of the anion by means of Fourier Transformation (FT) of velocity autocorrelation function and an Umbrella Sampling (US) calculation was made to quantify the interaction between the cation and anion.

2. Computational details

To investigate the structure and vibrational spectra of the pure liquids we considered three different simulation boxes, composed of 32 ion pairs each. For all the systems, a pre-equilibration was performed with classical molecular dynamics within periodic boundary conditions, using the AMBER [27] program package and the Gaff [28,29] force field. A 2-ns-long equilibration trajectory was produced for the systems in the NPT *ensemble*; the simulation temperature was set at 310 K. The difference between MD and experimental density was less than 5%. The edges (L) of the cubic cells are reported in Table 1 with the respective densities (ρ).

The final configurations of the classical trajectory were used as starting points for the *ab initio* molecular dynamics simulations, that were accomplished with the program package CP2K [30], using the Quickstep module [31] and the orbital transformation [32] for faster convergence. The electronic structure was calculated in the framework of Density Functional Theory [33,34], using the PBE [35] functional, with the explicit van der Waals terms according to the empirical dispersion correction

**Table 1.** Cubic cell edge (L), relative density (ρ) and energy drift (E_{drift}) of conserved quantity for ethylammonium nitrate (EAN), propylammonium nitrate (PAN), butylammonium nitrate (BAN).

Molecule	L (Å)	ρ (g/cm^3)	E_{drift} (a.u./fs)
EAN	18.01	1.21	$3.91*10^{-7}$
PAN	18.07	1.08	$5.76*10^{-7}$
BAN	19.21	1.07	$6.21*10^{-7}$

(D3) by Grimme [36]. Basis sets belonging to MOLOPT-DZVP-SR-GTH [37] family and GTH pseudopotentials [38,39] were applied; the time step chosen was 0.5 fs and the target temperature was set at 310 K by a Nosé-Hoover chain thermostat. After 7 ps of QM-equilibration, *NVT* trajectories of 50 ps were obtained. With the aim of checking the reliability of the AIMD, we calculated the relative energy drift (E_{drift}) of the 'conserved quantity' [30] during the production run. The obtained values are reported in Table 1. They reveal that the dynamics are stable and the chosen parameters for the thermostat and SCF criteria convergence are appropriate. In order to assess the free energy landscape of cation–anion interaction, we employed the US technique [40] on three smaller boxes composed of 10 ion pairs. In our model, a function of the collective variable N(Cat)···O(Ani) distance was chosen as bias, and we performed 36 constrained simulations overall, lasting 20 ps each. To make sure that the calculations worked correctly, we have analysed the histogram distribution of the restrained parameter. The separation between two consecutive windows was chosen as half of the full width at half maximum of the histogram, corresponding to 0.5 Å (see Figure 1 of Supporting Information). The unbiased probabilities of the collective variable were then easily recovered from the biased simulations using the weighted histogram analysis method (WHAM) [41]. The vibrational spectra were obtained from *ab initio* trajectories by calculating the vibrational density of states (VDOS) [42,43]. The assignment of each peak was performed using the MOLSIM [44] package. For this purpose, a set of internal coordinates (ICs) was defined and subsequently the Fourier transform of the velocity autocorrelation of all atoms was calculated and projected onto the effective normal modes [45,46], which are built as suitable linear combinations of ICs. As mentioned earlier, we are interested in the vibrational spectra of the anions because they are directly involved in the fingerprints of the hydrogen bond network of the complex. We have chosen the following ICs for our alkylammonium compounds: all the three N–O bonds, two distinct O–N–O angles and the out of plane deformation.

3. Results and discussion

The simplest structural patterns that can be extracted from an MD trajectory are the radial distribution functions (RDFs). Despite their simplicity, these are fundamental quantities because the Fourier transform of their combination [47] yields the total scattering functions that can be measured with a diffraction experiment (X-ray or neutron). We focus on the RDFs that reveal the two most important interactions of these ILs, namely the H-bond and dispersive interactions between alkyl chains. The
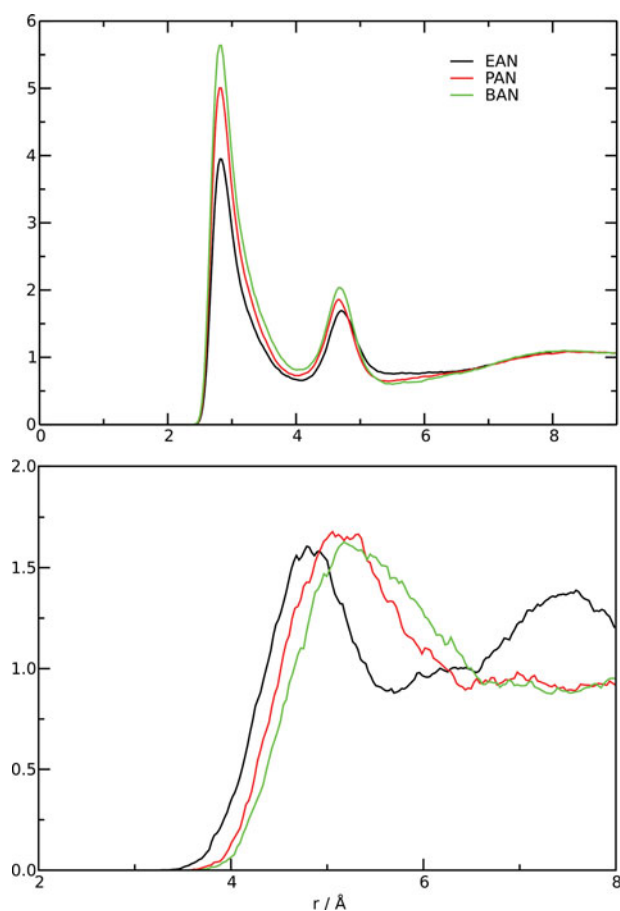
Figure 2. (Colour online) Top Panel: RDFs of N···O distance. Bottom Panel: RDFs between aliphatic chains COMs. In black the results obtained for ethylammonium nitrate (EAN), in red propylammonium nitrate (PAN) and in green butylammonium nitrate (BAN).

former is characterised by the N(Cat)···O(Ani), while the latter by the distance between the Centers of Mass (COMs) of the aliphatic chains. These RDFs are shown in Figure 2.

The present CP2K simulations clearly point to the first shell N···O distance around 2.8 Å for all ILs, a value which agrees with some of the previous data [11,13,48]. It can be inferred that the nitrate anion forms a strong hydrogen bond with the ammonium group of the cation. All ILs provide RDFs with the same peak positions, but the relative intensity increases with the alkyl chain length. Is is worth noting that the cation–anion equilibrium distance is not affected. The structure beyond the main peak that consists of one small peak around 4.7 Å is due to the tridentate nature of the anion that acts as HB acceptor. By looking at the bottom panel of Figure 2, we see that the alkyl chains originate a weak correlation, centred at about 4.2–4.6 Å. The equilibrium distance between the EAN alkyl chain COMs is shorter in comparison with the other ones, and can be related to

Table 2. H-bond analysis obtained from the AIMD simulation for ethylammonium nitrate (EAN), propylammonium nitrate (PAN), butylammonium nitrate (BAN).

| Molecule	N-coord	N–H bonds	$\tau 1$ (ps)	$\tau 2$ (ps)
EAN	3.73	2.23	1.21	0.12
PAN	4.86	2.56	1.28	0.13
BAN	5.34	2.65	1.52	0.15

the narrower dimension of its side chain. In this case the relative intensities of the RDFs are the same for all the curves.

In order to provide a quantitative description of the H-bond network we have reported in Table 2 the following properties: the number of oxygen atoms coordinated to the nitrogen atom of the cation (N-coord); the number of averaged H-bond like contacts (N-Hbonds) and the H-bonds lifetime ($\tau 1$ and $\tau 12$). The first parameter was calculated by fitting half a Gaussian function to the left part of the first peak and then doubling its area, that corresponds to the first coordination shell. The ILs do not show the same coordination number, it increases with the alkyl chain length (from 3.73 of EAN to 5.34 of BAN) . The second quantity was obtained with the VMD package [49]. The structural parameters (distance and angle) chosen to characterise the H-bond contacts are: the N···O distance, which ranges between 0 and 3.5 Å and the N−H···O angle from 135° to 180°. Even in this case there is a slight difference among the ILs. A long alkyl chain promotes the formation of H-bond contacts between the heteroatoms (N or O). Finally, H-bonds lifetime was considered as a subject of our study; for the calculation, we used TRAVIS autocorrelation function tool [50]. Figure 3 of Supporting Information shows the autocorrelation function for all the possible intermolecular hydrogen bonds. The points obtained were fitted using the function:

$$C(t) = Ae^{(-\frac{t}{\tau 1})} + (1-A)e^{(-\frac{t}{\tau 2})};\qquad(1)$$

where t is the time, A is a constant that determines the probability of the specific process, $\tau 1$ and $\tau 2$ are the characteristic times of the two processes. Process 1 ($\tau 1$), which is fast, is the breaking of the hydrogen bond itself, while the slower process 2 ($\tau 2$) is the migration of the IL pair outside the solvent cage. From Table 2, the EA···Nitrate hydrogen bond is the fastest to break ($\tau 1 = 1.21$ ps), while BAN presents the most stable hydrogen bond ($\tau 1 = 1.52$ ps). These observations can be explained in terms of the growing steric hindrance caused by the aliphatic moiety of the cation.

In order to provide three-dimensional information about the relative distribution of both the hydrophobic
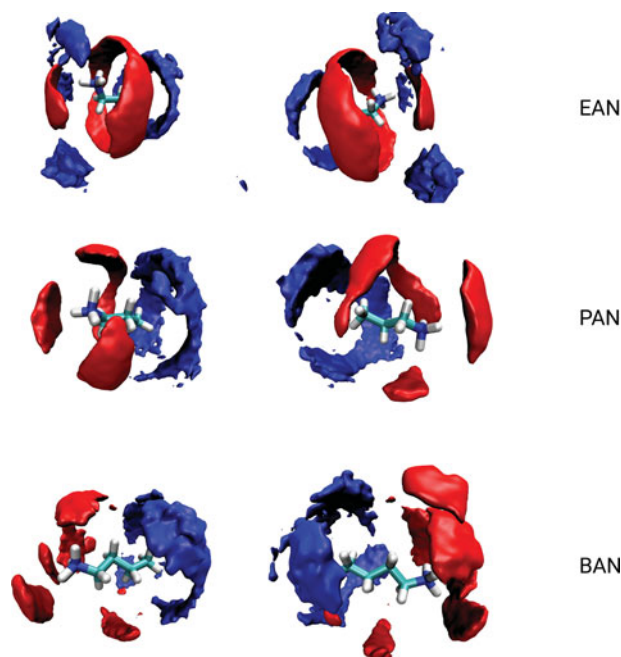

Figure 3. (Colour online) Spatial distribution function (SDF) of the anion center of mass (red) and alkyl chain (blue) around the cation for ethylammonium nitrate (EAN), propylammonium nitrate (PAN), butylammonium nitrate (BAN).

chain and the anions around the cations, we report in Figure 3 the Spatial Distribution Functions (SDFs); in each plot the isosurface contour was chosen to include half of the density. As it can be noted, in the first solvation shell around PAN and BAN cations, the anion centre of mass (red surface) and the alkyl chain (blue surface) are localised in two distinct areas. The former encloses the NH_3^+ group of the cation, while the latter surrounds the non-polar moiety of the molecule. This issue can be explained analogously to the hydrophobic effect: the non-polar substances aggregate in aqueous solution and exclude water molecules (in this case, the apolar part moves away from the polar heads) [51]. Unlike PAN and BAN, EAN exhibits a different pattern. Caused by its narrowness/shortness, the ethylammonium cation tail cannot entirely segregate from the anions. Hence, the ensuing isodensity plot is more homogeneous. This aspect endorses the previous results, namely the increasing sizes of alkyl chain encourages the approach of polar groups and stabilises the hydrogen bond interactions.

To study the vibrational properties of the liquids, we decided to use a 'dynamic approach' based on simulation trajectories. As a matter of fact, when the number of atoms in the molecular system increases, the number of local minima of the potential energy surface (PES) becomes quickly so large that a systematic search is impossible. Furthermore, the Hessian matrix diagonalisation calculation of the entire system would
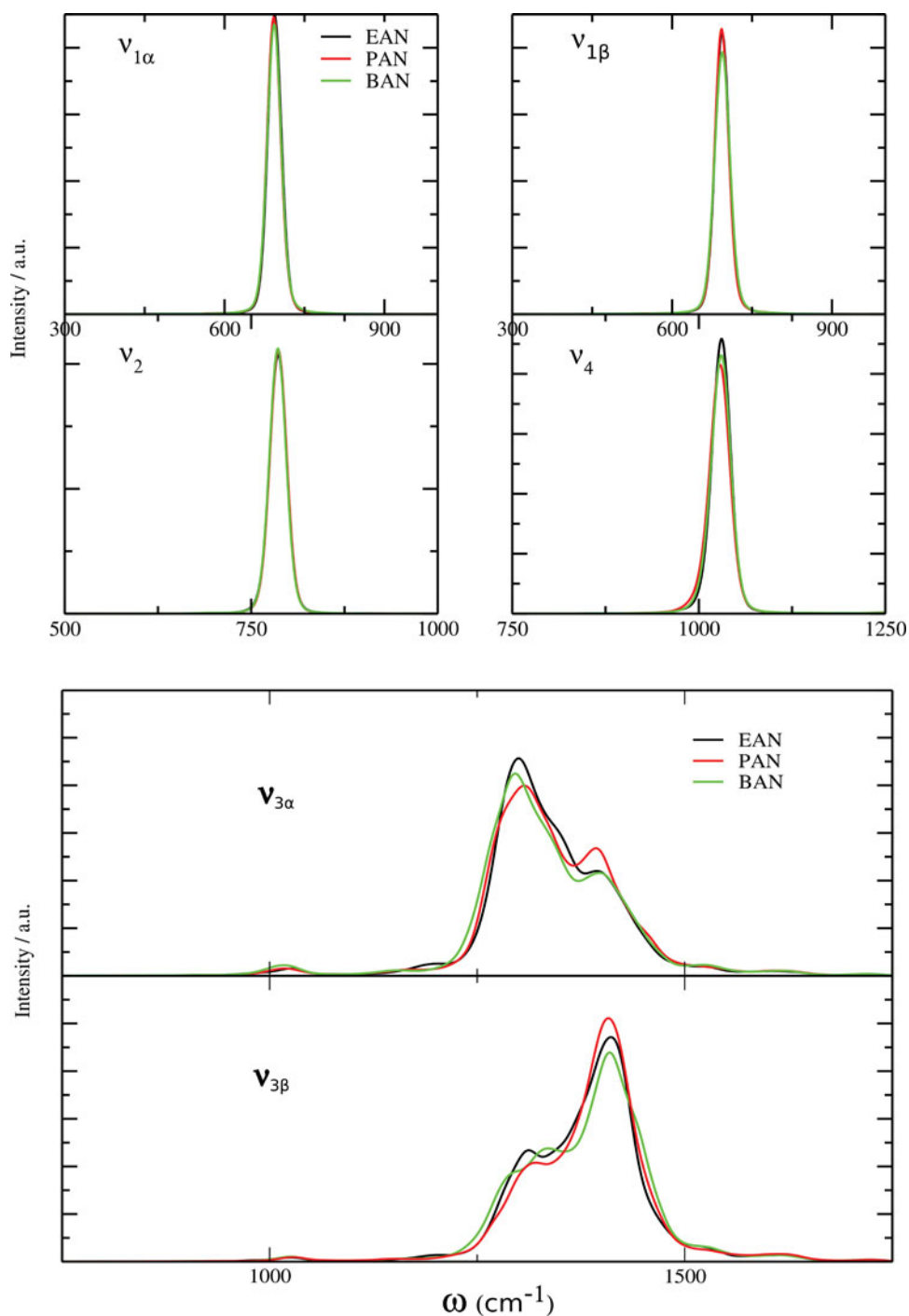
Figure 4. (Colour online) Velocity Density Of States (VDOS) of the nitrate anion six normal modes. In black the results obtained for ethylammonium nitrate (EAN), in red propylammonium nitrate (PAN) and in green butylammonium nitrate (BAN).

be computationally prohibitive. In other words, the large number of internal degrees of freedom prevents the use of standard static vibrational methods to extract the normal modes. The simplest way to obtain a vibrational spectrum from an AIMD trajectory is to calculate the power spectrum, since it only relies on the nuclear velocities, which are always known during a molecular dynamics simulation. For each atom, the velocity autocorrelation vector is calculated and the sum of all correlation functions of a molecule is Fourier transformed to get the power spectrum of that molecule. The procedure adopted to calculate the normal modes is explained in the computational section. The final normal modes are schematically represented in Figure 4 of Supporting Information, while the relative Velocity Density Of States (VDOS) are represented in Figure 4.

Table 3. Peak position for the splitted normal mode ν_3 for ethylammonium nitrate (EAN), propylammonium nitrate (PAN), butylammonium nitrate (BAN).

Molecule	Peak-1 (cm^{-1})	Peak-2 (cm^{-1})	Peak-1 (cm^{-1})	Peak-2 (cm^{-1})
EAN	1298	1389	1325	1418
PAN	1303	1392	1327	1420
BAN	1298	1393	1322	1415

The VDOS exhibits the following characteristics:

(1) The first two states ($\nu_{1\alpha}$ and $\nu_{1\beta}$) are degenerate for all the ILs, and they are associated with the bending mode of the O–N–O angle. They occur at about 700 cm^{-1}.

(2) The position and the relative intensity of the first four peaks ($\nu_{1\alpha}$, $\nu_{1\beta}$, ν_2 and ν_4) does not change with the alkyl chain length. This indicates that they are little affected by the hydrogen bond network as already observed in previous works [16,52].

(3) The ν_3 normal mode loses its degeneracy, owing to the hydrogen bond interaction between cation and anion. The resulting absorption can be expressed as a convolution of two distinct peaks.

To study in greater depth the splitting of the antisymmetric normal mode, we have performed a gaussian decomposition of the peaks of the relative VDOS. From this analysis we can determine the peak position in a more accurate way. The results are reported in Table 3.

It can be noticed that both VDOS show a similar splitting, which amounts to about 90 cm^{-1}. This value is in line with the results obtained for 2-OMeEAN [52]. So we can state that the combined effect of the hydrogen bond network and the symmetry breaking of the nitrate molecules leads to a partial splitting of the two antisymmetric stretching of the N–O bonds. Such phenomenon appears to be independent of the length of the cation organic moiety. The last study carried out on those compounds is an energy analysis of the cation–anion interaction. To quantify such interaction, we performed an US [53] calculation on the QM trajectories, using the N(Cat)$\cdots$O(Ani) distance as reaction coordinate. The resulting Potentials of Mean Force (PMF) [54], shown in Figure 5, have a Morse-like shape. The minima range from 3.7 kcal/mol for EAN to 4.4 kcal/mol for BAN, and all of them are located at 2.80 Å. Such values are weaker than the values reported for carboxylic acid dimers in [55–57] and for another class of ILs, obtained from amino acids [58]. It is remarkable to notice that the length of the alkyl chain does not influence the position of the minima. Conversely, it makes the cation–anion interaction
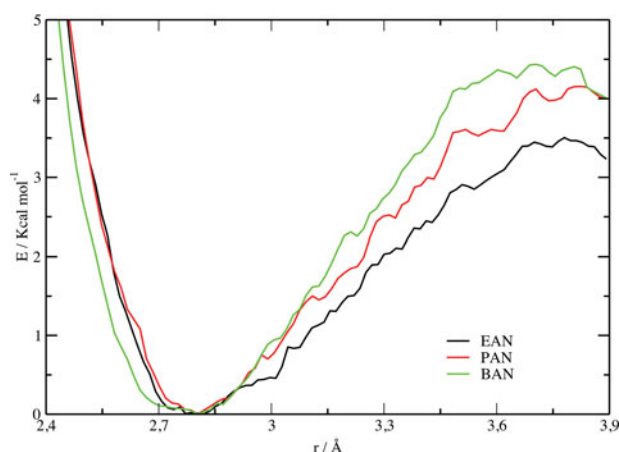
Figure 5. (Colour online) The Potential of Mean Force of the cation-anion interaction. The PMF is represented as a function of N(cat)$\cdots$O(ani) distance. In black the results obtained for ethylammonium nitrate (EAN), in red propylammonium nitrate (PAN) and in green butylammonium nitrate (BAN).

stronger. This is in line with the features observed in the RDFs.

4. Conclusions

In this work, the comparison among structural and dynamical properties of three protic ILs, 'ethylammonium nitrate, propylammonium nitrate and butylammonium nitrate', is reported. The aim of this work was to assess the effect of the alkyl chain length on the properties of such compounds. The hydrogen bond N$\cdots$O distance between cation and anion, calculated from the radial distribution functions from the *ab initio* trajectories, is 2.8 Å for the three ILs and it is in line with literature values, both experimental and theoretical. On the contrary, the relative intensities of the radial distribution functions change with the length of the side chain. Longer is the chain, more ions can be coordinated. This feature is also traceable in the hydrogen bonds lifetime. It is maximum for BAN, 1.52 ps, and minimum for EAN, 1.21 ps. Thanks to the projection of the VDOS onto collective variables, it was possible to distinguish the partial contribution of all the effective normal modes of the anion. It was shown how the different organic moieties do not have effects on the normal modes of the anions; in our

analysis, we have observed the same phenomena seen for the 2-methoxyethylammonium nitrate, namely the loss of degeneracy for the antisymmetric stretching normal modes. The last energetic analysis performed on the ILs shows that the intermolecular forces between cation and anion get stronger when the length of the alkyl chain is increased. But, as in the case of the radial distribution function, it does not affect the position of the minima in the potential of mean force landscape. All those aspects can be attributed to hydrophobic effects deriving from the interaction among the aliphatic chains of the cations. This condition increases with the size of cation's apolar moiety. Such hydrophobic interactions favours the hydrogen-bond contacts among the polar groups of the ILs. Hence PAN and BAN present more long-lasting and stable cation–anion interactions compared to EAN.

Acknowledgments

Disclosure statement

No potential conflict of interest was reported by the authors.

ORCID

M. Campetella 🟢 http://orcid.org/0000-0002-1853-6685

References

[1] J.S. Wilkes, Green. Chem. **4**(2), 73 (2002).
[2] E.W. Castner Jr and J.F. Wishart, J. Chem. Phys. **132**(12), 120901 (2010).
[3] P. Wasserscheid and W. Keim, Angew. Chem. Int. Ed. **39**(21), 3772 (2000).
[4] G.J. Kabo, A.V. Blokhin, Y.U. Paulechka, A.G. Kabo, M.P. Shymanovich, and J.W. Magee, J. Chem. Eng. Data **49**(3), 453 (2004).
[5] V. Kamavaram and R.G. Reddy, Int. J. Therm. Sci. **47**(6), 773 (2008).
[6] S. De Santis, G. Masci, F. Casciotta, R. Caminiti, E. Scarpellini, M. Campetella, and L. Gontrani, Phys. Chem. Chem. Phys. **17**(32), 20687 (2015).
[7] T.L. Greaves and C.J. Drummond, Chem. Rev. **108**(1), 206 (2008).
[8] K. Fumino, A. Wulf and R. Ludwig, Angew. Chem. Int. Ed. **48**(17), 3184 (2009).
[9] K. Fumino, A. Wulf, and R. Ludwig, Phys. Chem. Chem. Phys. **11**(39), 8790 (2009).
[10] K. Fumino, T. Peppel, M. Geppert-Rybczyńska, D.H. Zaitsau, J.K. Lehmann, S.P. Verevkin, M. Köckerling and R. Ludwig, Phys. Chem. Chem. Phys. **13**(31), 14064 (2011).
[11] E. Bodo, A. Sferrazza, R. Caminiti, S. Mangialardo, and P. Postorino, J. Chem. Phys. **139**(14), 144309 (2013).
[12] A. Mariani, R. Caminiti, M. Campetella, and L. Gontrani, Phys. Chem. Chem. Phys. **18**(4), 2297 (2016).
[13] M. Campetella, L. Gontrani, F. Leonelli, L. Bencivenni, and R. Caminiti, Chem. Phys. Chem. **16**(1), 197 (2015).
[14] V. Vchirawongkwin, C. Kritayakornupong, A. Tongraar, and B.M. Rode, J. Phys. Chem. B **115**(43), 12527 (2011).
[15] J. Thøgersen, J. Réhault, M. Odelius, T. Ogden, N.K. Jena, S.J.K. Jensen, S.R. Keiding, and J. Helbing, J. Phys. Chem. B **117**(12), 3376 (2013).
[16] E. Bodo, S. Mangialardo, F. Ramondo, F. Ceccacci, and P. Postorino, J. Phys. Chem. B **116**(47), 13878 (2012).
[17] S. Zahn, J. Thar, and B. Kirchner, J. Chem. Phys. **132**(12), 124506 (2010).
[18] V. Vchirawongkwin, C. Kritayakornupong, A. Tongraar, and B.M. Rode, J. Phys. Chem. B **115**(43), 12527 (2011).
[19] F. Ramondo, L. Tanzi, M. Campetella, L. Gontrani, G. Mancini, A. Pieretti, and C. Sadun, Phys. Chem. Chem. Phys. **11**(41), 9431 (2009).
[20] M. Campetella, L. Gontrani, E. Bodo, F. Ceccacci, F.C. Marincola, and R. Caminiti, J. Chem. Phys. **138**(18), 184506 (2013).
[21] L. Gontrani, E. Bodo, A. Triolo, F. Leonelli, P. D'Angelo, V. Migliorati, and R. Caminiti, J. Phys. Chem. B **116**(43), 13024 (2012).
[22] M. Campetella, E. Bodo, R. Caminiti, A. Martino, F. D'Apuzzo, S. Lupi, and L. Gontrani, J. Chem. Phys. **142**(23), 234502 (2015).
[23] M. Campetella, E. Bodo, M. Montagna, S. De Santis, and L. Gontrani, J. Chem. Phys. **144**(10), 104504 (2016).
[24] L. Tanzi, F. Ramondo, R. Caminiti, M. Campetella, A. Di Luca, and L. Gontrani, J. Chem. Phys. **143**(11), 114506 (2015).
[25] G. Prampolini, M. Campetella, N. De Mitri, P.R. Livotto, and I. Cacelli, J. Chem. Theor. Comput. **12**(11), 5525 (2016).
[26] M. Campetella, D.C. Martino, E. Scarpellini, and L. Gontrani, Chem. Phys. Lett. **660**, 99 (2016).
[27] R. Salomon-Ferrer, D.A. Case, and R.C. Walker, WIREs Comput. Mol. Sci. **3**(2), 198 (2013).
[28] J. Wang, R.M. Wolf, J.W. Caldwell, P.A. Kollman, and D.A. Case, J. Comput. Chem. **25**(9), 1157 (2004).
[29] J. Wang, W. Wang, P.A. Kollman, and D.A. Case, J. Mol. Graph. Mod. **25**(2), 247 (2006).
[30] J. Hutter, M. Iannuzzi, F. Schiffmann, and J. VandeVondele, WIREs Comput. Mol. Sci. **4**(1), 15 (2014).
[31] J. VandeVondele, M. Krack, F. Mohamed, M. Parrinello, T. Chassaing, and J. Hutter, Comput. Phys. Commun. **167**(2), 103 (2005).
[32] J. VandeVondele and J. Hutter, J. Chem. Phys. **118**(10), 4365 (2003).
[33] P. Hohenberg and W. Kohn, Phys. Rev. **136**(3B), B864 (1964).
[34] W. Kohn and L.J. Sham, Phys. Rev. **140**(4A), A1133 (1965).
[35] J.P. Perdew, K. Burke, and M. Ernzerhof, Phys. Rev. Lett. **77**(18), 3865 (1996).
[36] S. Grimme, J. Comput. Chem. **27**(15), 1787 (2006).
[37] J. VandeVondele and J. Hutter, J. Chem. Phys. **127**(11), 114105 (2007).

[38] S. Goedecker, M. Teter, and J. Hutter, Phys. Rev. B **54**(3), 1703 (1996).
[39] C. Hartwigsen, S. Gœdecker, and J. Hutter, Phys. Rev. B **58**(7), 3641 (1998).
[40] G.M. Torrie and J.P. Valleau, J. Comput. Phys. **23**(2), 187 (1977).
[41] S. Kumar, J.M. Rosenberg, D. Bouzida, R.H. Swendsen, and P.A. Kollman, J. Comput. Chem. **13**(8), 1011 (1992).
[42] M.P. Gaigeot, M. Martinez, and R. Vuilleumier, Mol. Phys. **105**(19–22), 2857 (2007).
[43] M. Martinez, M.P. Gaigeot, D. Borgis, and R. Vuilleumier, J. Chem. Phys. **125**(14), 144106 (2006).
[44] D. Bovi, A. Mezzetti, R. Vuilleumier, M.P. Gaigeot, B. Chazallon, R. Spezia, and L. Guidoni, Phys. Chem. Chem. Phys. **13**(47), 20954 (2011).
[45] D. Bovi, D. Narzi, and L. Guidoni, New J. Phys. **16**(1), 015020 (2014).
[46] G. Fogarasi, X. Zhou, P.W. Taylor, and P. Pulay, J. Am. Chem. Soc. **114**(21), 8191 (1992).
[47] D.A. Keen, J. Appl. Cryst. **34**(2), 172 (2001).
[48] R. Hayes, S. Imberti, G.G. Warr, and R. Atkin, Angew. Chem. Int. Ed. **51**(30), 7468 (2012).
[49] W. Humphrey, A. Dalke, and K. Schulten, J. Mol. Graph. **14**(1), 33 (1996).
[50] M. Brehm and B. Kirchner, J. Chem. Inf. Mod. **51**(8), 2007 (2011).
[51] D. Chandler, Nature **437**(7059), 640 (2005).
[52] M. Campetella, D. Bovi, R. Caminiti, L. Guidoni, L. Bencivenni, and L. Gontrani, J. Chem. Phys. **145**(2), 024507 (2016).
[53] G.M. Torrie and J.P. Valleau, J. Comput. Phys. **23**(2), 187 (1977).
[54] S. Kumar, J.M. Rosenberg, D. Bouzida, R.H. Swendsen, and P.A. Kollman, J. Comput. Chem. **16**(11), 1339 (1995).
[55] T. Neuheuser, B.A. Hess, C. Reutel, and E. Weber, J. Phys. Chem. **98**(26), 6459 (1994).
[56] Y. Gu, T. Kar, and S. Scheiner, J. Am. Chem. Soc. **121**(40), 9411 (1999).
[57] M.W. Feyereisen, D. Feller, and D.A. Dixon, J. Phys. Chem. **100**(8), 2993 (1996).
[58] M. Campetella, S. De Santis, R. Caminiti, P. Ballirano, C. Sadun, L. Tanzi, and L. Gontrani, RSC Adv. **5**(63), 50938 (2015).